

# Wavelength conversion for single-photon polarization qubits through continuous variable quantum teleportation

Xi-Wang Luo,<sup>1</sup> Chuanwei Zhang,<sup>1</sup> Irina Novikova,<sup>2</sup> Chen Qian,<sup>3</sup> and Shengwang Du<sup>1</sup>

<sup>1</sup>*Department of Physics, The University of Texas at Dallas, Richardson, Texas 75080-3021, USA*

<sup>2</sup>*Department of Physics, William and Mary, Williamsburg, VA 23187, USA*

<sup>3</sup>*Department of Computer Science and Engineering,  
University California Santa Cruz, Santa Cruz, CA 95064, USA*

A quantum internet connects remote quantum processors that need interact and exchange quantum signals over a long distance through photonic channels. However, these quantum nodes are usually composed of quantum systems with emitted photons unsuitable for long-distance transmission. Therefore, quantum wavelength conversion to telecom is crucial for long-distance quantum networks based on optical fiber. Here we propose wavelength conversion devices for single-photon polarization qubits using continuous variable quantum teleportation, which can efficiently convert qubits between near-infrared (780/795 nm suitable for interacting with atomic quantum nodes) and telecom wavelength (1300-1500 nm suitable for long-distance transmission). The teleportation uses entangled photon sources (i.e., non-degenerate two-mode squeezed state) that can be generated by four-wave mixing in rubidium atomic vapor cells, with a diamond configuration of atomic transitions. The entangled fields can be emitted in two orthogonal polarizations with locked relative phase, making them especially suitable for interfacing with single-photon polarization qubits. Our work paves the way for the realization of long-distance quantum networks.

## INTRODUCTION

Quantum technologies have been intensively developed in recent years [1–3]. In particular, long-distance quantum communication is crucial for unconditional security as well as connecting remote quantum processors through quantum internet [4, 5]. A quantum internet is expected to be more powerful than the simple sum of each quantum nodes, enabling a number of revolutionary applications such as quantum networks of clocks [6] and distributed quantum computing. Its realization will rely on the long-distance communication between remote quantum processors through photonic channels [4, 5]. However, single-photon qubits emitted from these quantum nodes (such as atomic ensembles [7], trapped ions [8]), often in the visible or near-infrared (NIR) regions, are usually unsuitable for long-distance transmission. Moreover, interconnections between disparate quantum systems was impossible due to their mismatched emission wavelengths [2, 4, 5, 9]. Quantum wavelength conversion (QWC) [10], which enables the spectral translation of a photon to targeted wavelength without disturbing its quantum properties, is a solution to these issues.

QWC between the NIR and telecom bands [11] is one of the most important wavelength conversions, since telecom band photons remain the information carrier of choice for long-distance transmission based on optical fiber, while the NIR photons not only interact with atomic quantum systems but also fall into the working band of many high-performance single-photon detectors [12] and quantum memories [13]. For long-distance communication between remote quantum nodes, one first uses the QWC device to convert the single-photon qubit emitted by quantum node *A* from NIR to telecom wave-

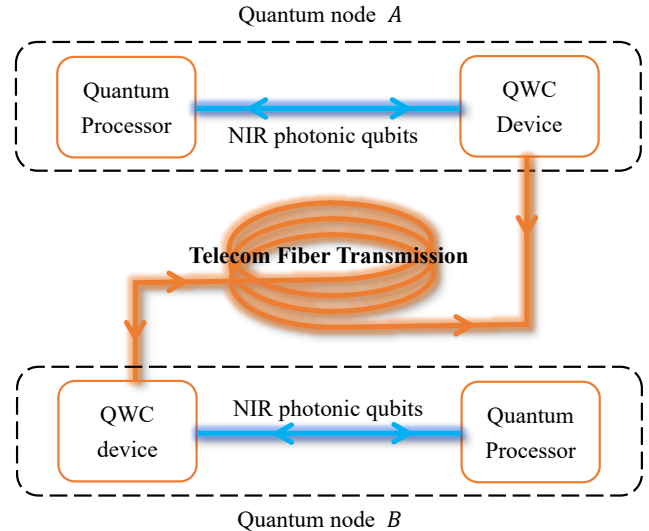


FIG. 1: Illustration of long-distance communication between remote quantum nodes.

length; then send it to quantum node *B* through fiber transmission; and finally convert its wavelength back to NIR band for interacting with the quantum processor (as illustrated in Fig. 1). QWC between NIR and telecom bands has been demonstrated for application to a wide range of quantum systems (e.g., trapped ions and rubidium gas) [14–21]. However, these QWC devices are usually based on three- or four-wave nonlinear optical mixing, which still has difficulty about noise photon and conversion efficiency (30% ~ 70%) to realize photonic interface.

In this paper, we propose wavelength conversion devices for single-photon polarization qubits using con-

tinuous variable (CV) quantum teleportation [22–25]. The entangled sources of the CV teleporters are non-degenerate two-mode squeezed vacuum (TMSV) states. By performing a joint homodyne measurement of a single photon and one of the entangled fields at the same NIR (telecom) wavelength, we can then teleport the single-photon qubit into the telecom (NIR) band, by imprinting the measured joint quadratures into the other entangled field at the shifted wavelength. The use of a hybrid technique involving CV teleportation of a discrete-variable (i.e., polarization qubits) allows deterministic wavelength conversion of photonic qubits with nearly 100% efficiency.

Since homodyne measurements [26] require using light of known polarization, therefore, two polarizations need to be teleported parallelly and each polarization component of the qubit requires a TMSV entangled state in the teleportation. Additional phase locking between the two polarization teleporters (i.e., the two TMSV entangled states) is necessary to avoid any phase errors in the teleportation, which is still challenging even for ordinary CV teleportation without wavelength conversion, where the degenerate TMSV entangled source is generated by mixing two identical single-mode squeezed states at a 50:50 beam splitter.

To realized QWC, we need to use *non-degenerate* TMSV states which cannot be generated by mixing single-mode squeezed states. We propose to generate the entangled source using a four-wave mixing (FWM) process in a hot Rubidium vapor cell with a diamond configuration of atomic transitions [27–30], in which the wavelength of one of the fields matches the single photon emitted from the atomic quantum nodes, and the other falls into the telecom-band optical fields, suitable for low loss fiber transmission. Because of the symmetry, the TMSV states can be emitted in two orthogonal polarizations with fixed relative phase, making them especially suitable for interfacing with polarization single photon qubits. Our approach provides an attractive alternative to a nonlinear crystal-based wavelength conversion that typically has low efficiency and requires tremendous technical care. In principle, the CV teleportation based wavelength conversion can be generalized to a wide range of frequencies as long as suitable two-color squeezed states can be generated using non-linear optical mixing.

## QWC THROUGH CV TELEPORTATION

Quantum teleportation [31] is a technique for transferring quantum information from a sender at one location to a receiver some distance away, by sending only classical information using a shared entangled state as a resource. It has become one of the key elements of advanced and practical quantum information protocols. Originally quantum teleportation was proposed for discrete variables qubit, and much progress has been

made in demonstrating quantum teleportation of photonic qubits. However, most of these schemes share one fundamental restriction: they require an unambiguous two-qubit Bell-state measurement which is always probabilistic (with a success probability 50%) when linear optics is used [32].

The concept was generalized to CV teleportation [22], which relies on the quadrature-entangled states (i.e., two-mode squeezed states) [33] and the measurements in the quadrature bases using linear optics and homodyne detection, leading to deterministic teleportation without post-selection. So far, the CV teleportation has been used to unconditionally teleport quantum states such as nonclassical CV state and time-bin qubits with fixed polarization [34–39]. Since homodyne measurements require light of known polarization, one need a pair of such entangled states with locked relative phase to parallelly teleport the two spin components of the qubits.

We consider non-degenerate two-mode squeezed states generated by the following Hamiltonian

$$H_{\text{sq}} = \sum_{s=H,V} [i\xi_s \hat{a}_{A,s}^\dagger \hat{a}_{B,s}^\dagger + h.c.], \quad (1)$$

which leads to squeezing between modes  $A$  and  $B$  for both polarizations  $H$  and  $V$ . Here  $\hat{a}_{A,B}^\dagger$  are the photon creation operators of modes  $A$  and  $B$ , with corresponding frequencies  $\omega_{A,B}$  falling in the NIR and telecom bands respectively. The entangled source  $|\text{ES}\rangle = e^{-iH_{\text{sq}}\tau}|\text{vac}\rangle$  is generated by evolving the vacuum under the Hamiltonian  $H_{\text{sq}}$  for certain time period  $\tau$ . We obtain a pair of two-mode squeezed vacuum  $|\text{ES}\rangle_\Omega = \prod_s \hat{S}_s(r_s)|\text{vac}\rangle$ , with  $\hat{S}_s(r) = e^{r\hat{a}_{A,s}^\dagger \hat{a}_{B,s}^\dagger - h.c.}$  the two-mode squeezing operator [33, 40] for polarization  $s$  and  $r_s = \xi_s \tau$  the squeezing factor. We assume  $r_H = r_V = r$  are real, therefore, a pair of in-phase non-degenerate TMSV states are generated coherently.

In the photon number basis, the entangled source can be written as [25]

$$\begin{aligned} |\text{ES}\rangle &= (1 - q^2) \sum_{n,m} q^{n+m} |n; m\rangle_A |n; m\rangle_B \\ &= (1 - q^2) \sum_{n,N} q^N |n; N - n\rangle_A |n; N - n\rangle_B \end{aligned} \quad (2)$$

where  $|n; N - n\rangle$  represents  $n$  photons in  $H$  polarization and  $N - n$  photons in  $V$  polarization, and  $q = \tanh(r)$ . We want to teleport a single-photon polarization qubit  $|\psi\rangle_{\text{in}} = c_1|1; 0\rangle_{\text{in}} + c_2|0; 1\rangle_{\text{in}}$  and convert its frequency from  $\omega_A$  to  $\omega_B$ .

The quantum wavelength conversion device based on CV teleportation process is schematically illustrated in Fig. 2. First, we combine the input mode with mode  $A$  at a half beam splitter and make the balanced homodyne detection of mode  $\hat{a}_{\pm,s} = \frac{\hat{a}_{\text{in},s} \pm \hat{a}_{A,s}}{\sqrt{2}}$  with  $\hat{a}_{\text{in},s}$  the input field operator for polarization  $s$ . We use a local oscillator

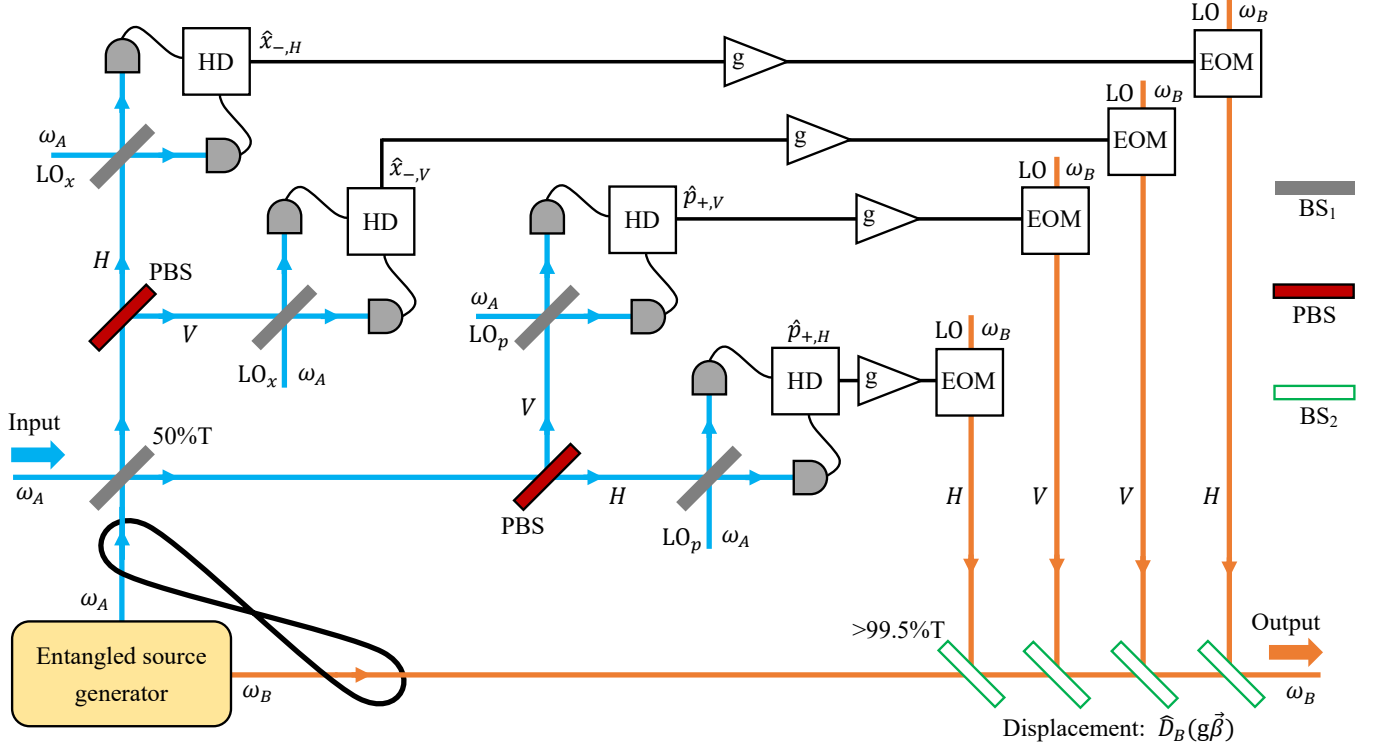


FIG. 2: Schematic illustration of the quantum wavelength conversion device based on CV quantum teleportation. BS<sub>1</sub> and BS<sub>2</sub> represent the beam splitters with 50% and >99.5% transmittance, respectively; PBS, HD and EOM represent polarizing beam splitter, homodyne detector and electro-optic modulator. LO<sub>x</sub> and LO<sub>p</sub> are local oscillators to measure  $x$  and  $p$  quadratures, respectively. For the homodyne detection (displacement), the frequencies of local oscillators are  $\omega_A$  ( $\omega_B$ ).

with frequency  $\omega_A$  to measure  $\hat{x}_{-,s} = (\hat{a}_{-,s} + \hat{a}_{-,s}^\dagger)/\sqrt{2}$  and  $\hat{p}_{+,s} = i(\hat{a}_{+,s}^\dagger - \hat{a}_{+,s})/\sqrt{2}$ , which generates the control signal  $\vec{\beta} = (\beta_H, \beta_V)$ , where  $\beta_s = \langle \hat{x}_{-,s} + i\hat{p}_{+,s} \rangle$  and  $\langle \cdot \rangle$  corresponds to the detection projection. The homodyne measurement projects the state of input and  $A$  modes to the state

$$|\vec{\beta}\rangle_{\text{in},A} = \frac{1}{\pi} \sum_{n,m} \hat{D}_{\text{in}}(\vec{\beta}) |n; m\rangle_{\text{in}} |n; m\rangle_A \quad (3)$$

with displacement operator  $\hat{D}_{\text{in}}(\vec{\beta}) = \prod_s e^{\beta_s \hat{a}_{\text{in},s}^\dagger - \beta_s^* \hat{a}_{\text{in},s}}$ . Then we perform the displacement  $g\vec{\beta}$  on mode  $B$  using a local oscillator with frequency  $\omega_B$ , and accomplish the teleportation. Here  $g$  is the gain factor and the output state (unnormalized) in mode  $B$  becomes

$$\begin{aligned} |\psi\rangle_{\text{out}} &= {}_{\text{in},A} \langle \vec{\beta} | \hat{D}_B(g\vec{\beta}) | \text{ES} \rangle |\psi\rangle_{\text{in}} \\ &= \hat{T}_q(\vec{\beta}) |\psi\rangle_{\text{in}}, \end{aligned} \quad (4)$$

where

$$\hat{T}_q(\vec{\beta}) = \frac{1-q^2}{\pi} \sum_{n,m} q^{n+m} \hat{D}_B(g\vec{\beta}) |n; m\rangle_B {}_{\text{in}} \langle n; m | \hat{D}_{\text{in}}(-\vec{\beta})$$

is the transfer operator. In the strong squeezing limit, we have  $\hat{T}_q(\vec{\beta}) \propto \sum_{n,m} |n; m\rangle_B {}_{\text{in}} \langle n; m |$  for unit gain  $g = 1$ ,

and the normalized output state reads

$$|\psi\rangle_{\text{out}} = c_1 |1; 0\rangle_B + c_2 |0; 1\rangle_B, \quad (5)$$

which is identical to the input state, except that the frequency of the qubit is shifted from  $\omega_A$  to  $\omega_B$ . The teleportation process corresponds to one-photon teleportation in  $H$  ( $V$ ) polarization and a vacuum teleportation in  $V$  ( $H$ ) polarization. Similarly, we can convert the wavelength of the photonic qubit from  $\omega_B$  to  $\omega_A$ .

To generate the displacement on mode  $B$ , we can use electro-optical modulators (EOMs) to modulate the local oscillator (the local oscillator has frequency  $\omega_B$ ) according to the homodyne detection signals, and combine these phase modulated beams with mode  $B$  at a beam splitter of >99.5% transmittance (as shown in Fig. 2). Moreover, we want to mention that the ideal two-mode squeezing requires infinite energy, and ideal CV entangled source is physically unattainable; thus, the teleportation fidelity is generally limited by the squeezing factor. In this case, non-unit gain conditions are useful [39, 41, 42]. With proper choice of the gain factor  $g = q = \tanh(r)$ , no additional photons would be created in the output, and the teleported single photon qubit remains undisturbed regardless of the squeezing level, with a success probability  $q^2$  [39, 41, 42]. Therefore, the wavelength conversion efficient (i.e.,  $q^2$ ) can be nearly 100% for sufficiently strong

squeezing  $\tanh(r) \rightarrow 1$ .

### ENTANGLED SOURCE FROM FWM

The key element of our scheme is to generate a pair of non-degenerate TMSV states, where the wavelength of one mode in the TMSV state matches photons emitted from the quantum nodes, and the other mode falls into the telecom band. In this section, we show how to generate such non-degenerate two-mode squeezing through four-wave mixing.

As we discussed previously, homodyne measurements require using light of known polarization, therefore, two polarizations need to be teleported parallelly and each polarization component of the qubit requires a TMSV entangled state. The relative phase between the two TMSV states should be locked. Suppose there is a random and unknown relative phase between the two polarizing TMSV states (i.e., we replace  $\hat{a}_{A,V}$  and  $\hat{a}_{B,V}$  by  $e^{-i\phi_A}\hat{a}_{A,V}$  and  $e^{-i\phi_B}\hat{a}_{A,V}$  in Eq. 1), then the entangled state becomes

$$|\text{ES}(\phi)\rangle = (1 - q^2) \sum_{n,m} q^{n+m} e^{im\phi} |n; m\rangle_A |n; m\rangle_B$$

with  $\phi = \phi_A + \phi_B$  a random and unknown phase. The final output state becomes

$$|\psi(\phi)\rangle_{\text{out}} = c_1 |1; 0\rangle_B + c_2 e^{i\phi} |0; 1\rangle_B \quad (6)$$

with a phase error. Therefore, even the ordinary CV teleportation (without wavelength conversion) of a single-photon polarization qubit is still challenging and has not been demonstrated experimentally, since a TMSV state generated by mixing two identical single-mode squeezed states usually has an unknown relatively phase with respect to other TMSV states generated in the same way.

To realized QWC through CV teleportation, we need to use non-degenerate TMSV states which cannot be generated by mixing single-mode squeezed states. Here we consider the four-wave mixing in a hot Rubidium vapor cell [27–30, 43, 44], with a diamond configuration of atomic transitions, as shown in Fig. 3a. The ground state  $5S_{1/2}$  is coupled to the excited state  $4D_{3/2}$  through a two-photon process, with intermediate states  $5P_{1/2}$  or  $5P_{3/2}$ . The setup is schematically shown in Fig. 3b. An ensemble of  $^{87}\text{Rb}$  atoms is trapped with a magneto-optical trap, all atoms are initialized to ground state  $5S_{1/2}$ . In the FWM process, two pump lasers (with NIR wavelength  $\lambda_1 = 795$  nm and telecom  $\lambda_2 = 1475$  nm, respectively) are used to excite atoms to state  $4D_{3/2}$  with intermediate state  $5P_{1/2}$ . Then state  $4D_{3/2}$  decays back to  $5S_{1/2}$  through parametric down conversion with intermediate state  $5P_{3/2}$ , followed by the generation of photon pairs (with telecom wavelength  $\lambda_B = 1529$  nm and NIR wavelength  $\lambda_A = 780$  nm, respectively). The Hamiltonian of

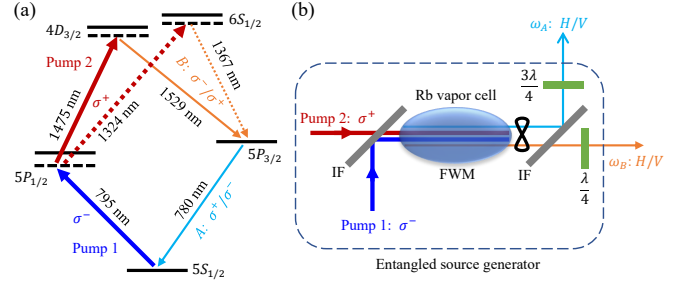


FIG. 3: Illustration of the FWM process to generate two-mode squeezing. (a) Level scheme for the FWM in  $^{87}\text{Rb}$ . (b) Schematic of the proposed entangled source generator. IF represents the interference filter. The  $\frac{3\lambda}{4}$  and  $\frac{\lambda}{4}$  waveplates are used to convert  $\sigma^\pm$  to  $H/V$  polarizations.

the FWM process can be written as

$$H_{\text{FWM}} = \chi^{(3)} \hat{a}_1 \hat{a}_2 \hat{a}_A^\dagger \hat{a}_B^\dagger + h.c., \quad (7)$$

where  $\chi^{(3)}$  is the third-order nonlinear coefficient and  $a_j$  is the annihilation operator for optical field  $\lambda_j$ . We can replace the field operator  $\hat{a}_{1,2}$  of the pump lasers by the coherent amplitudes  $\hat{\alpha}_{1,2}$ , then  $H_{\text{FWM}} \rightarrow i\xi \hat{\alpha}_A^\dagger \hat{\alpha}_B^\dagger + h.c.$  with  $\xi = -i\chi^{(3)} \hat{\alpha}_1 \hat{\alpha}_2$  to be real for proper gauge choice. Energy conservation requires that the generated photon pairs in mode  $A$  and  $B$  have frequencies  $\omega_A$  and  $\omega_B$ , respectively, where  $\omega_j = \frac{2\pi c}{\lambda_j}$  satisfies  $\omega_A + \omega_B = \omega_1 + \omega_2$  and  $c$  is the speed of light.

Now we examine the polarizations of the two-mode squeezing fields generated by FWM. We consider that the four fields are in a co-propagating geometry inside the atomic cloud, which satisfies the phase matching, as shown in Fig. 3b. With the quantization axis along the beam propagation direction of all modes, we drive transitions with  $\Delta m_F = \pm 1$  using two pump beams that are orthogonally circularly polarized. In the coherent parametric down conversion process, the final quantum state of the atoms remains the same as the initial state. Furthermore, rotational symmetry of the atomic cloud along beam propagation direction implies angular momentum conservation. The angular momentum selection rules limit the polarizations of the generated photon pairs, and the Hamiltonian becomes

$$H_{\text{FWM}} = i\xi (\hat{a}_{A,\sigma^+}^\dagger \hat{a}_{B,\sigma^-}^\dagger - s \hat{a}_{A,\sigma^-}^\dagger \hat{a}_{B,\sigma^+}^\dagger + h.c.), \quad (8)$$

where  $\sigma^\pm$  denote the left and right circular polarizations, respectively, and  $s$  is determined by the Clebsch-Gordan coefficients [29]. We can choose the initial state as  $5S_{1/2}$ ,  $F = 2$ ,  $m_F = 0$ , which leads to  $s = 1$ . Therefore, with proper local operations on the entangled fields  $\hat{a}_{A,\sigma^\pm} \rightarrow \hat{a}_{A,HV}$  and  $\hat{a}_{B,\sigma^\mp} \rightarrow \hat{a}_{B,HV}$ ,  $H_{\text{FWM}}$  reduces to  $H_{\text{sq}}$  and the FWM process generates two-mode squeezing for both polarizations with locked and known relative phase, which makes them especially suitable for teleporting single-photon polarization qubits.

We want to point out that, the parametric down conversion process may have multi decay paths through different hyperfine levels of  $5P_{3/2}$ , we can use additional filters to select one decay path (e.g.,  $5P_{3/2}$ ,  $F = 3$ ). We can also use  $\lambda_1 = 780$ ,  $\lambda_2 = 1529$  for the pump beams with  $5P_{3/2}$  the corresponding intermediate state, then we obtain the two-mode squeezing with wavelength  $\lambda_A = 795$  and  $\lambda_B = 1475$ . Moreover, we can choose a different atomic level such as  $6S_{1/2}$  to be the high excited state (see Fig. 3a), which allows us to generate telecom fields with wavelength 1324 nm and 1367 nm.

## FINITE QUBIT BANDWIDTH

We have assumed a single-frequency photonic qubit in the discussion above, while in practice, the photonic qubit always has a finite frequency bandwidth. In the Heisenberg picture, the balanced homodyne detection corresponds to projection measurement  $\beta_s(t) = \langle e^{i\omega_A t} \hat{a}_{\text{in},s}(t) - e^{-i\omega_A t} \hat{a}_{A,s}^\dagger(t) \rangle$ . After performing the displacement on mode  $B$ , the output fields are

$$\hat{a}_{\text{out},s}(t) = \hat{a}_{B,s}(t) + e^{-i\omega_- t} \hat{a}_{\text{in},s}(t) - e^{-i\omega_+ t} \hat{a}_{A,s}^\dagger(t), \quad (9)$$

with  $\omega_\pm = \omega_B \pm \omega_A$ . In the frequency domain, we have

$$\begin{aligned} \hat{a}_{\text{out},s}(\omega_B + \Omega) &= \hat{a}_{\text{in},s}(\omega_A + \Omega) \\ &+ \hat{a}_{B,s}(\omega_B + \Omega) - \hat{a}_{A,s}^\dagger(\omega_A - \Omega). \end{aligned} \quad (10)$$

This means that, we need two-mode squeezing between frequency component  $\omega_A - \Omega$  in mode  $A$  and the frequency component  $\omega_B + \Omega$  in mode  $B$  to convert a single-frequency qubit from  $\omega_A + \Omega$  to  $\omega_B + \Omega$ .

Meanwhile, we can take into account the finite squeezing bandwidth of the FWM process, and the Hamiltonian reads

$$H_{\text{FWM}} = i\xi \sum_{s,\Omega} [\hat{a}_{A,s}^\dagger(\omega_A - \Omega) \hat{a}_{B,s}^\dagger(\omega_B + \Omega) + h.c.] \quad (11)$$

due to energy conservation, with  $\Omega$  taking values within the squeezing bandwidth. The Hamiltonian in Eq. 11 leads to exactly the desired squeezing. In the Heisenberg picture, the TMSV state satisfies  $[\hat{a}_{B,s}(\omega_B + \Omega) - \hat{a}_{A,s}^\dagger(\omega_A - \Omega)]_{\text{TMSV}} = e^{-r} [\hat{a}_{B,s}(\omega_B + \Omega) - \hat{a}_{A,s}^\dagger(\omega_A - \Omega)]_{\text{vac}}$ . In the strong squeezing limit, the output field Eq. 10 becomes exactly the same as the input field  $\hat{a}_{\text{out},s}(\omega_B + \Omega) = \hat{a}_{\text{in},s}(\omega_A + \Omega)$ , except the frequency is shifted by  $\omega_B - \omega_A$ . Therefore, our proposal works as long as the squeezing bandwidth is sufficiently wide to cover the qubit bandwidth.

## DISCUSSION AND CONCLUSION

We have shown how to realize the wavelength conversion for single-photon polarization qubits through CV

teleportation, and to generalize the two-mode squeezed entangled source using FWM. For long-distance communication between remote quantum nodes, we can use the procedure as illustrated in Fig. 1. Alternatively, we can first send telecom mode of the entangled source from node  $A$  to node  $B$ ; then teleport the photonic qubit from node  $A$  to  $B$  with wavelength conversion; and finally convert the qubit back to NIR wavelength at node  $B$ . For the later approach, additional photon loss may be introduced to the entangled source during the transmission, which will reduce the teleportation fidelity [45].

In summary, we proposed a QWC device for single-photon polarization qubits using continuous variable quantum teleportation. We considered a four-wave mixing process in rubidium atomic vapor cell with a diamond configuration of atomic transitions to generate the entangled source, which corresponds to a pair of in-phase non-degenerate TMSV states. One of the entangled fields has wavelength 780/795 nm and the other has wavelength 1300-1500 nm, allowing efficiently wavelength conversion of single-photon qubits between NIR (suitable for interacting with atomic quantum nodes) and telecom-wavelength (suitable for long-distance transmission). Moreover, it is possible to generate the wavelength conversion scheme to a wide range of frequencies as long as the corresponding two-color squeezed states can be generated by suitable non-linear optical mixing. Our work provides an attractive alternative to a nonlinear crystal-based wavelength conversion that still has difficulty about noise photon and conversion efficiency.

## ACKNOWLEDGEMENT

X.W.L. and C.Z. are supported by AFOSR (FA9550-20-1-0220), NSF (PHY-1806227), and ARO (W911NF-17-1-0128). S.D. acknowledges the Texas STARs and Start-Up fundings from The University of Texas at Dallas. I.N. is supported by AFOSR (FA9550-19-1-0066). C.Q. was supported by NSF (CNS-1750704 and CPS-1932447).

- 
- [1] Y. Alexeev *et al.*, Development of Quantum Interconnects (QuICs) for Next-Generation Information Technologies, *PRX Quantum* **2**, 017001 (2021).
  - [2] D. Awschalom *et al.*, Development of Quantum Interconnects (QuICs) for Next-Generation Information Technologies, *PRX Quantum* **2**, 017002 (2021).
  - [3] E. Altman *et al.*, Quantum Simulators: Architectures and Opportunities, *PRX Quantum* **2**, 017003 (2021).
  - [4] H. J. Kimble, The quantum internet, *Nature* **453**, 1023 (2008).
  - [5] S. Wehner, D. Elkouss, R. Hanson, Quantum internet: A vision for the road ahead, *Science* **362**, eaam9288 (2018).

- [6] P. Komar, E. M. Kessler, M. Bishof, L. Jiang, A. S. Sørensen, J. Ye, and M. D. Lukin, A quantum network of clocks, *Nature* **10**, 582 (2014).
- [7] L.-M. Duan, M. D. Lukin, J. I. Cirac, and P. Zoller, Long-distance quantum communication with atomic ensembles and linear optics, *Nature* **414**, 413 (2001).
- [8] L.-M. Duan and C. Monroe, Colloquium: Quantum networks with trapped ions, *Rev. Mod. Phys.* **82**, 1209 (2010).
- [9] M. Wallquist, K. Hammerer, P. Rabl, M. Lukin, and P. Zoller, Hybrid quantum devices and quantum engineering, *Phys. Scr.* **T137**, 014001 (2009).
- [10] P. Kumar, Quantum frequency conversion, *Opt. Lett.* **15**, 1476 (1990).
- [11] S. Tanzilli, W. Tittel, M. Halder, O. Alibart, P. Baldi, N. Gisin, and H. Zbinden, A photonic quantum information interface, *Nature* **437**, 116 (2005).
- [12] R. H. Hadfield, Single-photon detectors for optical quantum information applications, *Nat. Photon.* **3**, 696 (2009).
- [13] N. Sangouard, C. Simon, H. de Riedmatten, and N. Gisin, Quantum repeaters based on atomic ensembles and linear optics, *Rev. Mod. Phys.* **83**, 33 (2011).
- [14] R. Ikuta, Y. Kusaka, T. Kitano, H. Kato, T. Yamamoto, M. Koashi, and N. Imoto, Wide-band quantum interface for visible-to-telecommunication wavelength conversion, *Nat. Commun.* **2**, 537 (2011).
- [15] A. Radnaev, Y. O. Dudin, R. Zhao, H. H. Jen, S. Jenkins, A. Kuzmich, and T. A. B. Kennedy, A quantum memory with telecom-wavelength conversion, *Nat. Phys.* **6**, 894 (2010).
- [16] Y. O. Dudin, A. G. Radnaev, R. Zhao, J. Z. Blumoff, T. A. B. Kennedy, and A. Kuzmich, Entanglement of Light-Shift Compensated Atomic Spin Waves with Telecom Light, *Phys. Rev. Lett.* **105**, 260502 (2010).
- [17] T. Walker, K. Miyaniishi, R. Ikuta, H. Takahashi, S. V. Kashanian, Y. Tsujimoto, K. Hayasaka, T. Yamamoto, N. Imoto, and M. Keller, Long-Distance Single Photon Transmission from a Trapped Ion via Quantum Frequency Conversion, *Phys. Rev. Lett.* **120**, 203601 ((2018)).
- [18] M. Bock, P. Eich, S. Kucera, M. Kreis, A. Lenhard, C. Becher, and J. Eschner, High-fidelity entanglement between a trapped ion and a telecom photon via quantum frequency conversion, *Nat. Commun.* **9**, 1998 (2018).
- [19] Y. Yu *et al.*, Entanglement of two quantum memories via fibres over dozens of kilometres, *Nature* **578**, 240 (2020).
- [20] N. Maring, P. Farrera, K. Kutluer, M. Mazzer, G. Heinze, and H. de Riedmatten, Photonic quantum state transfer between a cold atomic gas and a crystal, *Nature* **551**, 485 (2017).
- [21] R. Ikuta, T. Kobayashi, T. Kawakami, S. Miki, M. Yabuno, T. Yamashita, H. Terai, M. Koashi, T. Mukai, T. Yamamoto, and N. Imoto, Polarization insensitive frequency conversion for an atom-photon entanglement distribution via a telecom network, *Nat. Commun.* **9**, 1997 (2018).
- [22] L. Vaidman, Teleportation of quantum states, *Phys. Rev. A* **49**, 1473 (1994).
- [23] Samuel L. Braunstein and H. J. Kimble, Teleportation of Continuous Quantum Variables, *Phys. Rev. Lett.* **80**, 869 (1998).
- [24] A. Furusawa, J. L. Sørensen, S. L. Braunstein, C. A. Fuchs, H. J. Kimble, and E. S. Polzik, Unconditional Quantum Teleportation, *Science* **282**, 706 (1998).
- [25] T. Ide, H. F. Hofmann, T. Kobayashi, and A. Furusawa, Continuous-variable teleportation of single-photon states, *Phys. Rev. A* **65**, 012313 (2001).
- [26] H. Wiseman and G. Milburn, *Quantum Measurement and Control* (Cambridge University Press, Cambridge, 2010).
- [27] T. Chanelière, D. N. Matsukevich, S. D. Jenkins, T. A. B. Kennedy, M. S. Chapman, and A. Kuzmich, Quantum Telecommunication Based on Atomic Cascade Transitions, *Phys. Rev. Lett.* **96**, 093604 (2006).
- [28] B. Srivathsan, G. K. Gulati, B. Chng, G. Maslennikov, D. Matsukevich, and C. Kurtsiefer, Narrow Band Source of Transform-Limited Photon Pairs via Four-Wave Mixing in a Cold Atomic Ensemble, *Phys. Rev. Lett.* **111**, 123602 (2013).
- [29] G. K. Gulati, B. Srivathsan, B. Chng, A. Cerè, and C. Kurtsiefer, Polarization entanglement and quantum beats of photon pairs from four-wave mixing in a cold  $^{87}\text{Rb}$  ensemble, *New J. Phys.* **17**, 093034 (2015).
- [30] K. Wang, S. Shi, W. Zhang, Y. Ye, Y. Yu, M. Dong, Y. Zhai, D. Ding, and B. Shi, Experimental demonstration of two-color Einstein-Podolsky-Rosen entanglement in a hot vapor cell, *OSA Continuum* **2**, 2260 (2019).
- [31] C. H. Bennett, G. Brassard, C. Crépeau, R. Jozsa, A. Peres, and W. K. Wootters, Teleporting an unknown quantum state via dual classical and Einstein-Podolsky-Rosen channels, *Phys. Rev. Lett.* **70**, 1895 (1993).
- [32] J.-W. Pan, Z.-B. Chen, C.-Y. Lu, H. Weinfurter, A. Zeilinger, and M. Żukowski, Multiphoton entanglement and interferometry, *Rev. Mod. Phys.* **84**, 777 (2012).
- [33] A. I. Lvovsky, Squeezed light, [arXiv:1401.4118](https://arxiv.org/abs/1401.4118).
- [34] W. P. Bowen, N. Treps, B. C. Buchler, R. Schnabel, T. C. Ralph, H.-A. Bachor, T. Symul, and P. K. Lam, Experimental investigation of continuous-variable quantum teleportation, *Phys. Rev. A* **67**, 032302 (2003).
- [35] X. Jia, X. Su, Q. Pan, J. Gao, C. Xie, and K. Peng, Experimental Demonstration of Unconditional Entanglement Swapping for Continuous Variables, *Phys. Rev. Lett.* **93**, 250503 (2004).
- [36] N. Takei, H. Yonezawa, T. Aoki, and A. Furusawa, High-Fidelity Teleportation beyond the No-Cloning Limit and Entanglement Swapping for Continuous Variables, *Phys. Rev. Lett.* **94**, 220502 (2005).
- [37] H. Yonezawa, S. L. Braunstein, and A. Furusawa, Experimental Demonstration of Quantum Teleportation of Broadband Squeezing, *Phys. Rev. Lett.* **99**, 110503 (2007).
- [38] N. Lee, H. Benichi, Y. Takeno, S. Takeda, J. Webb, E. Huntington, A. Furusawa, Teleportation of Nonclassical Wave Packets of Light, *Science* **332**, 330 (2011).
- [39] S. Takeda, T. Mizuta, M. Fuwa, P. van Loock, and A. Furusawa, Deterministic quantum teleportation of photonic quantum bits by a hybrid technique, *Nature* **500**, 315 (2013).
- [40] D. F. Walls and G. J. Milburn, *Quantum optics* (Springer-Verlag, Berlin, 2008).
- [41] H. F. Hofmann, T. Ide, T. Kobayashi, and A. Furusawa, Information losses in continuous-variable quantum teleportation, *Phys. Rev. A* **64**, 040301(R) (2001).
- [42] R. E. S. Polkinghorne and T. C. Ralph, Continuous variable entanglement swapping, *Phys. Rev. Lett.* **83**, 2095 (1999).

- [43] M. Dabrowski, M. Parniak, and W. Wasilewski, Einstein-Podolsky-Rosen paradox in a hybrid bipartite system, *Optica* **4**, 272 (2017).
- [44] N. Prajapati and I. Novikova, Polarization-Based Truncated SU(1,1) Interferometer based on Four-wave Mixing in Rb vapor, *Opt. Lett.* **44**, 5921 (2019).
- [45] S. H. Lie and H. Jeong, Limitations of teleporting a qubit via a two-mode squeezed state, *Photon. Res.* **7**, A7 (2019).